Kidney International, Vol. 54 (1998), pp. 1240–1249

Nature of glomerular dysfunction in pre-eclampsia[1]

Richard A. Lafayette, Maurice Druzin, Richard Sibley, Geraldine Derby, Tahira Malik, Phil Huie, Catherine Polhemus, William M. Deen, and Bryan D. Myers

Departments of Medicine, Obstetrics, and Pathology, Stanford University Medical Center, Stanford University School of Medicine, Stanford, California, and Department of Chemical Engineering, Massachusetts Institutes of Technology, Cambridge, Massachusetts, USA

Nature of glomerular dysfunction in pre-eclampsia.

Background. Pre-eclampsia is characterized by hypertension, proteinuria and edema. Simultaneous studies of kidney function and structure have not been reported. We wished to explore the degree and nature of glomerular dysfunction in pre-eclampsia.

Methods. Physiologic techniques were used to estimate glomerular filtration rate (GFR), renal plasma flow and afferent oncotic pressure immediately after delivery in consecutive patients with pre-eclampsia (PET; $N = 13$). Healthy mothers completing an uncomplicated pregnancy served as functional controls ($N = 12$). A morphometric analysis of glomeruli obtained by biopsy and mathematical modeling were used to estimate the glomerular ultrafiltration coefficient (K_f). Glomeruli from healthy female kidney transplant donors served as structural controls ($N = 8$).

Results. The GFR in PET was depressed below the control level, 91 ± 23 versus 149 ± 34 ml/min/1.73 m^2, respectively ($P < 0.0001$). In contrast, renal plasma flow and oncotic pressure were similar in the two groups (P = NS). A reduction in the density and size of endothelial fenestrae and subendothelial accumulation of fibrinoid deposits lowered glomerular hydraulic permeability in PET compared to controls, 1.81 versus 2.58 × 10^{-9} m/sec/PA. Mesangial cell interposition also curtailed effective filtration surface area. Together, these changes lowered the computed single nephron K_f in PET below control, 4.26 versus 6.78 nl/min · mm Hg, respectively.

Conclusion. The proportionate (~40%) depression of K_f for single nephrons and GFR suggests that hypofiltration in PET does not have a hemodynamic basis, but is a consequence of structural changes that lead to impairment of intrinsic glomerular ultrafiltration capacity.

Pre-eclamptic toxemia (PET) is characterized by gestational hypertension, a phenomenon that has been attributed to an excess of vasoconstrictor over vasodilator influences in the systemic circulation [1–5]. A parallel imbalance in the renal circulation would be expected to lower the glomerular perfusion rate. Another characteristic of PET is abnormal glomerular morphology [6–8], which could lower the intrinsic ultrafiltration capacity of glomerular capillaries. Limited glomerular ultrafiltration capacity on its own, or more particularly, in combination with glomerular underperfusion, is predicted to result in depression of the glomerular filtration rate (GFR). Yet, as judged by elevation of serum creatinine concentration to abnormal levels, depression of GFR is a sufficiently infrequent finding that it is not used as a criterion for the diagnosis of PET [9–11].

The absence of azotemia, usually defined in females as a serum creatinine concentration >1.2 mg/dl, does not exclude a substantial PET-mediated reduction in GFR, however. GFR during the second half of pregnancy, when PET is likely to become manifest, is normally elevated above non-gravid levels by ~50% [12–14]. A reciprocal decline in the serum creatinine level is typically to only ~0.6 mg/dl, on average [13, 15]. Further, the relationship between GFR and serum creatinine concentration is hyperbolic, that is, a given percent reduction from high levels of the former would result in a proportionately smaller percent increase in the latter [16]. Thus, for serum creatinine to exceed 1.2 mg/dl as a result of PET would require a >50% depression of GFR from prevailing gravid levels.

A major goal of the present study was to confirm that PET indeed lowers the GFR, albeit insufficiently in most cases to result in overt azotemia. A second goal was to elucidate possible mechanisms by which PET lowers the GFR. To accomplish this, we used a combination of physiologic and morphometric techniques and mathematical modelling to evaluate individual determinants of the GFR in subjects with PET. Our findings form the basis of this report.

METHODS

Patient populations

Our experimental group comprised 13 of 15 consecutively consenting mothers diagnosed with PET because of the development of gestational hypertension and proteinuria during the second-half of pregnancy [11]. Gestational hypertension was defined as systolic and diastolic pressures

[1] **See *Editorial* by Chapman, p. 1394.**

Key words: pregnancy, GFR, renal blood flow, endothelial cell, biopsy, ultrafiltration coefficient, PET, gestational hypertension.

Received for publication January 5, 1998
and in revised form April 20, 1998
Accepted for publication April 28, 1998

in excess of 140 and 90 mm Hg respectively, in subjects not known to have pregestational hypertension. Proteinuria was defined as 2^+ by dipstick. Each recruited subject was asked, but not required, to undergo a renal biopsy during the first 48 postpartum hours. Of the ten subjects who consented to the performance of a biopsy, only eight had a constellation of histopathological changes typical of pure PET. One of the remaining subjects was found to have acute postinfectious glomerulonephritis, with endocapillary cell proliferation and subepithelial, electron dense, "hump-like" deposits. The other was found to have idiopathic focal and segmental glomerulosclerosis with chronic renal damage. Changes of PET in endothelial cells and subendothelial fibrinoid deposits were absent. These two latter patients were excluded from further analysis. The likelihood that each of the remaining 13 subjects indeed had PET was enhanced by the subsequent demonstration six weeks postpartum that both the gestational hypertension and the proteinuria had resolved.

Two groups of subjects served as controls. Twelve healthy women completing an uncomplicated pregnancy served as gravid controls. They provided reference values for the physiological determinations of interest during the first 24 postpartum hours. The PET and gravid control groups were similar in age, averaging 34 ± 2 (mean ± SD) and 30 ± 1 year, respectively (P = NS). The second control group was comprised of 8 healthy, female kidney transplant donors in their reproductive years. Each underwent a renal biopsy at the time of transplantation to provide control values for the morphometric analysis of glomerular structure in PET. All members of the two control groups denied a history of renal disease, hypertension or diabetes mellitus. At the time of evaluation, each was found to be normotensive and normoglycemic, to have a normal serum creatinine level, and to have a urinary protein excretion rate within the normal range.

Physiological evaluation

Our observations were made in the early postpartum period. Glomerular filtration dynamics were evaluated by a clearance technique, beginning 4.5 ± 0.9 and 4.3 ± 1.1 hour after delivery by cesarean section in the subjects of the PET and gravid control groups, respectively. We opted to study postcesarean patients because the routine use of a bladder catheter under these conditions permitted accurate measurement of the urine flow rate and avoided contamination of the urine sample by lochia. All subjects of both groups were receiving i.v. Pitocin (oxytocin) at the time of study.

A priming dose of inulin (50 mg/kg) and para-aminohippuric acid (PAH, 12 mg/kg) was administered. Thereafter, inulin and PAH were given by continuous infusion to maintain plasma levels constant at 20 and 1.5 mg/dl, respectively. Sixty minutes after the priming infusion, arterial blood pressure was determined by Dynamap, and blood was sampled for examination of plasma oncotic pressure (π_A) and plasma albumin concentration. Four consecutive 30-minute urine samples were then carefully collected, each bracketed by a blood sample drawn from a peripheral vein. The GFR was expressed as the average value for the four timed inulin clearances. The rate of renal plasma flow (RPF) in the subjects with PET was determined by dividing the corresponding clearance of PAH by an estimate of the renal arteriovenous extraction ratio for PAH (E_{PAH}). The value for E_{PAH} in each individual was estimated from a quadratic regression model that uses the prevailing GFR and post-glomerular oncotic pressure to derive E_{PAH} in subjects with glomerular disease [17]. According to this model, E_{PAH} averaged 0.76 and 0.90 in subjects with PET and controls, respectively. The extent of albuminuria was evaluated by determining the albumin-to-creatinine ratio in the first of the timed urine collections.

The concentrations of inulin and PAH were determined with an automated assay [16, 17]. Concentrations of albumin in serum and urine were determined by immunochemical methods and plasma oncotic pressure by membrane osmometry as described previously [18]. The oncotic pressure in systemic plasma was taken to be the same as that entering the afferent glomerular arteriole (π_A). Efferent oncotic pressure (π_E) was calculated as:

$$\pi_E = \pi_A/(1 - FF) \qquad \text{(Eq. 1)}$$

where FF is filtration fraction (GFR/RPF). Assuming that the axial rise in oncotic pressure along the glomerular capillaries is linear, we then computed the mean intraluminal glomerular oncotic pressure (π_{GC}) as the arithmetic mean of π_A and π_E [18].

Renal biopsy

Renal biopsy of the pre-eclamptic mothers was performed within 48 hours following delivery. Two cores were taken with a 16-gauge biopsy gun needle (Bard Monopty, Covington, GA, USA) under ultrasonic guidance. The first core and the central portion of the second core were prepared for light and transmission electron microscopy respectively, as described previously [19]. The two remaining outer portions of the second core were prepared for scanning electron microscopy (SEM), using a modification of the method of Shirato et al [20]. Briefly, freshly biopsied kidney tissue was immediately fixed in 4% glutaraldehyde in PBS, pH 7.4, and stored at 4°C. Before post-fixation, the samples were examined with a stereoscope. A cut was made near or through glomeruli in the samples. The samples were then washed in 0.1 M sodium cacodylate followed by three complete cycles of: a two hour post-fixation with 1% osmium tetroxide, a 20 minute wash with sodium cacodylate buffer, two hours of incubation in 1% tannic acid, and a 20-minute sodium cacodylate buffer wash. The samples were then dehydrated in a series of alcohols, immersed in hexamethylsilisane and allowed to dry thoroughly in a

dessiccator. The samples were finally placed on aluminum stubs, coated with gold, observed with a Philips 505 scanning electron microscope, and rotated and tilted to allow examination of glomerular endothelial surfaces *en face*. The images were recorded on Polaroid film.

Morphometric evaluation

All glomeruli in a single 1 μm paraffin-embedded section stained with periodic acid-Schiff reagent were analyzed at the light microscopic level. On average, 21 (range 6 to 41) glomeruli were examined in the biopsy material from subjects with PET. The average number of glomeruli among the control biopsies was 23 (range 9 to 62). A dedicated computer system (Southern Micro Instruments, Inc., Atlanta, GA, USA), consisting of a video camera, screen, microscope and digitizing tablet, was used to perform measurements. The outline of each glomerular tuft in the cross-section was traced onto the digitizing tablet at 900 $\times$ and the tuft cross-sectional area (A_G) computed from a polygon that was fitted to its outline as described by Weibel and Gomez [21]. Glomerular volume (V_G) was then calculated from A_G as follows:

$$V_G = \frac{\beta}{d}(A_G)^{3/2}(f_s f_i)^{-3} \qquad \text{(Eq. 2)}$$

where β is a dimensionless "shape coefficient" ($\beta = 1.38$ for spheres), d is a "size distribution coefficient," which is introduced to account for variations in glomerular size [21] and f_s and f_i are correction factors for the tissue shrinkage associated with paraffin embedding and immersion fixation, respectively. We used $d = 1.1$ as in previous studies [19, 22], which corresponds to a distribution of glomerular sizes with a SD of ~25% of the mean size [21]. We have determined that the value of the shrinkage factors in our embedding procedure and during immersion fixation are $f_s = 0.86$ and $f_i = 0.85$, respectively [22, 23].

Two or three Epon-embedded glomeruli centrally located within the block were randomly chosen from each biopsy and thin-sectioned (70 nm) for examination by TEM. Montage micrographs of full glomerular profiles ($\times$2820) were prepared for measurement by point and intercept counting of "effective" filtering surface density (S_v) of the peripheral glomerular capillary wall (GCW). In the past we have defined S_v as the length density of the peripheral GBM from mesangial junction to mesangial junction [19, 22]. Among the changes that characterized PET, however, were mesangial cell interposition and hypertrophy of endothelial cell bodies (*vide infra*). The part of the GBM that was apposed to these aforementioned structures was excluded on the grounds that transcellular filtration is negligible, and this component was designated "ineffective" filtration surface density. For purposes of the present study therefore, "effective" filtration surface density was defined as the remaining length density of peripheral GBM, that is, that which is apposed to the endothelial cytoplasmic rim.

Six-eight sections of each randomized glomerular profile were then photographed at $\times$11,280 to evaluate the dimensions of the filtration barrier. The frequency of filtration slits was determined by counting the total number of epithelial filtration slits and dividing it by the total length of the peripheral glomerular basement membrane (GBM) captured on the electron photomicrographs. The harmonic mean thickness of the filtering GBM (δ_{bm}) and separately, of the entire glomerular capillary wall (δ_{gcw}, that is, the interval of the filtration pathway from fenestrae to slit diaphragms) was then calculated using the orthogonal intercept method of Jensen [24]. In controls $\delta_{bm} = \delta_{gcw}$. In subjects with PET, however, $\delta_{gcw} > \delta_{bm}$, with the excess reflecting subendothelial fibrinoid deposits that lay free between the endothelial fenestrae and the lamina rara interna of the GBM (*vide infra*). Finally, scanning electron microscopy was used to characterize endothelial fenestral dimensions. Polaroid photographs of endothelial surfaces were digitized on a flat bed scanner by adjusting the (grey scale) image threshold. Three random areas, each of 1 μm^2, were then defined to serve as reference areas. Micrographs ($\times$20,000) taken normal to the plane of exposed endothelium ("en face") were used to determine fenestral density by manual counting. Higher magnification ($\times$50,000) was next used to calculate the size of all fenestrae in the reference area, and the fraction of underlying and filtering GBM occupied by fenestrae using the NIH Image program (version 1.45).

Calculation of the glomerular ultrafiltration coefficient

Single nephron (SN) K_f was calculated from the product of filtration surface area (S) and an estimate of the hydraulic permeability of the walls of glomerular capillaries (k) in the 2 to 3 glomeruli examined ultrastructurally. S was first calculated from:

$$S = S_v \times V_G(f_i f_s) \qquad \text{(Eq. 3)}$$

where S_v and V_G are respectively the mean values for "effective" peripheral capillary surface density and glomerular volume in each biopsy core.

The hydraulic permeability of the capillary wall (k) was estimated from the filtration slit frequency, basement membrane thickness (δ_{bm}), glomerular capillary wall thickness (δ_{gcw}), number of fenestrae per unit area of endothelial surface (n_f), and fenestral area/perimeter ratio using the ultrastructural-hydrodynamic model of Drumond and Deen [25]. In the model, the normal capillary wall is represented as consisting of a large number of repeating structural units, each of which is based on a single filtration slit. The width of a structural unit (W) is calculated as:

$$W = \frac{2}{\pi} \times \frac{1}{FSF} \qquad \text{(Eq. 4)}$$

where FSF is the filtration slit frequency and $2/\pi$ is a correction factor that accounts for the random angle of sectioning. The overall hydraulic permeability is related to the permeabilities of the individual layers by:

$$k = \left(\frac{1}{k_{en}} + \frac{1}{k_{bm}} + \frac{1}{k_{ep}}\right)^{-1} \quad \text{(Eq. 5)}$$

where k_{en}, k_{bm} and k_{ep} are the hydraulic permeabilities of the endothelium, basement membrane, and epithelium, respectively.

The endothelial permeability is given by:

$$k_{en} = \epsilon_f k_f \quad \text{(Eq. 6)}$$

where ϵ_f is the fraction of the capillary surface occupied by fenestrae and k_f is the permeability of a single fenestra. In addition to changes in the number density of fenestrae, ϵ_f is influenced by the size of an individual fenestra. The characteristic linear dimension of a fenestra is proportional to the area of the opening divided by its perimeter; the area-perimeter ratio is denoted as L. Hydrodynamically, the fenestrae may be viewed as orifices in a thin wall. Dimensional analysis of the equations for flow through an orifice at low Reynolds number indicates that the hydraulic permeability of the orifice is given by cL/μ, where c is a dimensionless constant that depends on the orifice shape and μ is the viscosity of the fluid. Thus, for flow of water through orifices of similar shape but differing size, the hydraulic permeability is predicted to vary in proportion to L.

The effective permeability of the basement membrane is governed by a relationship of the form:

$$k_{bm} = \frac{K_D}{\mu\delta_{bm}} f\left(\frac{W}{\delta_{bm}}, N_f, \epsilon_f, \epsilon_s\right) \quad \text{(Eq. 7)}$$

where k_D is the Darcy permeability and δ_{bm} is the thickness of the GBM, μ is the viscosity of water, N_f is the number of fenestrae per structural unit, ϵ_s is the fraction of the basement membrane area occupied by filtration slits, and the function f is given by equation 23 of Drumond and Deen [25]. The fractional slit area is given by $\epsilon_s = W_s/W$, where W_s is the width of a filtration slit at the level of the slit diaphragm. On the basis of the reduction in fenestral number density (n_f) in PET, the number of fenestrae per repeating unit (N_f) was reduced from 3 (the control value) to 2. The quantities K_D and W_s were estimated using literature data for rats as detailed previously [19, 22]. In PET, however, only part of glomerular capillary wall thickness is accounted for by GBM; the remainder is comprised of subendothelial fibrinoid material (*vida infra*). Not only is the Darcy permeability (K_D) of the latter material not known, but in the absence of knowledge of its precise composition it is not yet possible to measure its K_D *in vitro*. We accordingly resorted to a limited sensitivity analysis and examined the effects of variations of K_D for this "non-GBM" fraction on k_{bm}. We solved equation (7) for PET by assigning values of K_D that are either negligible (that is, fibrinoid imposes no resistance to water flow), or the same as the *in vitro* estimate for GBM. In the former instance only actual δ_{bm} was considered, whereas in the latter instance the thickness of the entire filtration pathway (δ_{gcw}) was substituted for δ_{bm} in equation (7).

Finally, the epithelial permeability was computed as:

$$k_{ep} = \epsilon_s k_s = \frac{W_s}{W} k_s \quad \text{(Eq. 8)}$$

where k_s is the permeability of the slit diaphragm, as estimated previously based on structural data for the rat [25].

Table 1. Clinical features

	Controls	PET
Age *years*	30 ± 1	34 ± 2
Gestational age *weeks*	39 ± 1	34 ± 5[a]
Infant birth weight *kg*	3.7 ± 3.0	1.9 ± 0.9[a]
Mean arterial pressure *mm Hg*	81 ± 6	104 ± 12[a]
Serum creatinine *mg/dl*	0.60 ± 0.10	0.83 ± 0.22[a]
Urine albumin:creatinine *mg/g*	32 ± 10	2810 ± 89[a]

Data are mean ± SD.
[a] $P < 0.05$, PET vs. controls

Statistical analysis

All results, except for the urinary albumin excretion rate, are expressed as the mean ± ISD. Student's *t*-test was used to test the significance of differences between the PET and corresponding control groups.

RESULTS

Clinical features

The appearance of dipstick proteinuria and the required level of hypertension (>140/>90 mm Hg), preceded delivery in the PET group by 5.7 ± 5.8 and 4.4 ± 4.9 days, respectively. At the time of examination in the immediate wake of delivery, the PET group differed from the healthy gravid control group in three respects: (*1*) the period of gestation was shorter, 34 ± 5 versus 39 ± 1 week ($P < 0.05$); (*2*) infant birth weight was lower, 1.9 ± 0.9 versus 3.7 ± 3.0 Kg ($P = 0.0004$), a difference that indicates immaturity as well as prematurity in the former; and (*3*) all subjects with PET were receiving treatment with $MgSO_4$ and in two instances, with nifedipine, whereas no group 2 subject received $MgSO_4$ or antihypertensive drugs. Despite the latter therapy, mean arterial pressure was significantly higher in PET than in the gravid controls, averaging 104 ± 12 versus 81 ± 6 mm Hg, respectively ($P < 0.001$, Table 1). The urinary albumin/creatinine ratio was also significantly greater in PET than in gravid controls (Table 1).

Table 2. Renal hemodynamics

	Controls	PET
Glomerular filtration rate *ml/min/1.73 m²*	149 ± 34	91 ± 25[a]
Renal plasma flow *ml/min/1.73 m²*	624 ± 108	648 ± 257
Filtration fraction *%*	24 ± 5	16 ± 5[a]
Afferent oncotic pressure (π_A) *mm Hg*	17.6 ± 1.3	17.0 ± 2.7
Glomerular oncotic pressure (π_{GC}) *mm Hg*	20.4 ± 1.7	18.6 ± 3.2

Data are mean ± SD.
[a] $P < 0.05$, PET vs. controls

Filtration dynamics

Similar to the observations of others during late pregnancy, the GFR in our gravid control subjects was elevated above normal non-gravid levels by ~50%, averaging 149 ± 34 ml/min/1.73 m^2 [12, 14, 15, 26]. We have thus demonstrated that pregnancy-associated hyperfiltration persists into the first postpartum day. When compared to this high value, the corresponding GFR in PET was significantly depressed, averaging only 91 ± 25 ml/min/1.73 m^2 ($P <$ 0.001, Table 2). Of note, the corresponding levels of serum creatinine in the control and PET groups were 0.60 ± 0.10 and 0.83 ± 0.22 mg/dl, respectively ($P < 0.001$, Table 1). Because of the hyperbolic relationship between this quantity and GFR, the highest serum creatinine in the PET group was only 1.2 mg/dl, despite simultaneous depression of corresponding GFR to 44 ml/min/1.73 m^2.

Unlike the GFR, renal plasma flow in gravid controls was not elevated above normal non-gravid levels, averaging 624 ± 108 ml/min/1.73 m^2. The corresponding renal plasma flow in the PET group was similar averaging 648 ± 257 ml/min/1.73 m^2 (P = NS, Table 2). The selective decline in PET of GFR resulted in marked depression of the filtration fraction, 16 ± 5 versus 24 ± 5% in controls ($P < 0.001$, Table 1). This latter finding indicates that determinants of GFR other than renal plasma flow must have been altered to explain the observed level of hypofiltration in PET.

A consistently reported finding of hypoalbuminemia in pregnancy has been attributed to a combination of hypervolemia (hemodilution) and altered protein metabolism [27–31]. We found serum albumin concentration to be markedly depressed in both groups, slightly more so in PET than gravid controls, 1.87 ± 0.20 versus 1.95 ± 0.22 g/dl, respectively (P = NS). The corresponding oncotic pressure of preglomerular plasma (π_A) varied in parallel, 17.0 ± 2.7 versus 17.6 ± 1.3 mm Hg (Table 2). Reflecting the lower filtration fraction in PET, we calculate that the disparity in oncotic pressure along the glomerular capillaries grew larger, such that π_{GC} averaged 18.6 ± 3.2 versus 20.4 ± 1.7 mm Hg in the gravid controls. The difference failed narrowly to reach statistical significance ($P = 0.07$). However, since π_{GC} is the force opposing the formation of filtrate, the trend towards depression of this quantity should have enhanced ultrafiltration pressure and hence, increased GFR [32]. It follows that depression of either the glomerular transcapillary hydraulic pressure difference and/or the glomerular ultrafiltration coefficient (K_f) must be invoked to explain the hypofiltration observed in PET.

Glomerular structure and morphometry

Examination by light microscopy revealed prominence of endocapillary (mesangial and endothelial) cells. There was conspicuous endothelial cellularity in most cases, evidenced by up to three endothelial cell nuclei in some capillary lumens. Definite mesangial hypercellulartiy was difficult to discern. There was also a prominent infiltration of macrophages and a lesser number of lymphocytes and polymorphonuclear leukocytes within capillary lumens in four of the cases. The hypertrophy of endothelial cells alone, or in combination with leukocyte infiltrates, resulted in obvious loss of capillary patency in all seven cases by light microscopy. Foamy macrophages were appreciated in two of the cases. There also was variable thickening of glomerular capillary walls. This appeared to be related to mesangial interposition in all cases, and prominent subendothelial hyaline deposits in one case. An additional finding was the presence of early focal segmental glomerular sclerosis in four out of seven of the individuals, affecting 19 ± 11% of glomeruli, on average. Examination by transmission electron microscopy confirmed the finding of endothelial cell hyperplasia, as well as that of exudation of foamy macrophages, lymphocytes and polymorphonuclear leukocytes within the capillary lumina and mesangium. In addition, capillary wall abnormalities that are illustrated and schematized in Figures 1 and 2, respectively, were apparent. These included: (*1*) hypertrophied endothelial cells; (*2*) swollen segments of endothelial cytoplasmic rim in which fenestrae were not discernible; (*3*) subendothelial fibrinoid and granular deposits; and (*4*) interposition of mesangial cells.

Glomerular volume in PET was significantly larger than in controls, 5.23 ± 2.16 versus 3.29 ± 1.19 $\mu m^3 \times 10^6$, respectively ($P < 0.05$, Table 3). As stated previously, we defined "effective" filtration surface as that part of the peripheral GBM that was apposed to the fenestrated endothelial cytoplasmic rim. The remaining part of the peripheral GBM that was apposed to endothelial cell bodies or interposed mesangial cells (numbers 1 and 4, respectively, Fig. 2) was excluded on the grounds that transcellular filtration is negligible. This latter component, which comprised the "ineffective" filtration surface density, was increased by a factor of 3 in PET versus controls (0.024 ± 0.001 vs. 0.008 ± 0.001, $\mu m^2/\mu m^3$, $P = 0.001$), mostly as a consequence of interposed mesangial cells. As a result, effective S_v was reduced in PET versus controls, averaging 0.055 ± 0.002 versus 0.100 ± 0.013, $\mu m^2/\mu m^3$ ($P < 0.001$, Table 3). However, a trend to larger glomerular volume in PET offset the reduction in S_v. As a result, actual filtration surface area calculated from equation (3) in PET was reduced below control by only 10% (P = NS, Table 4).

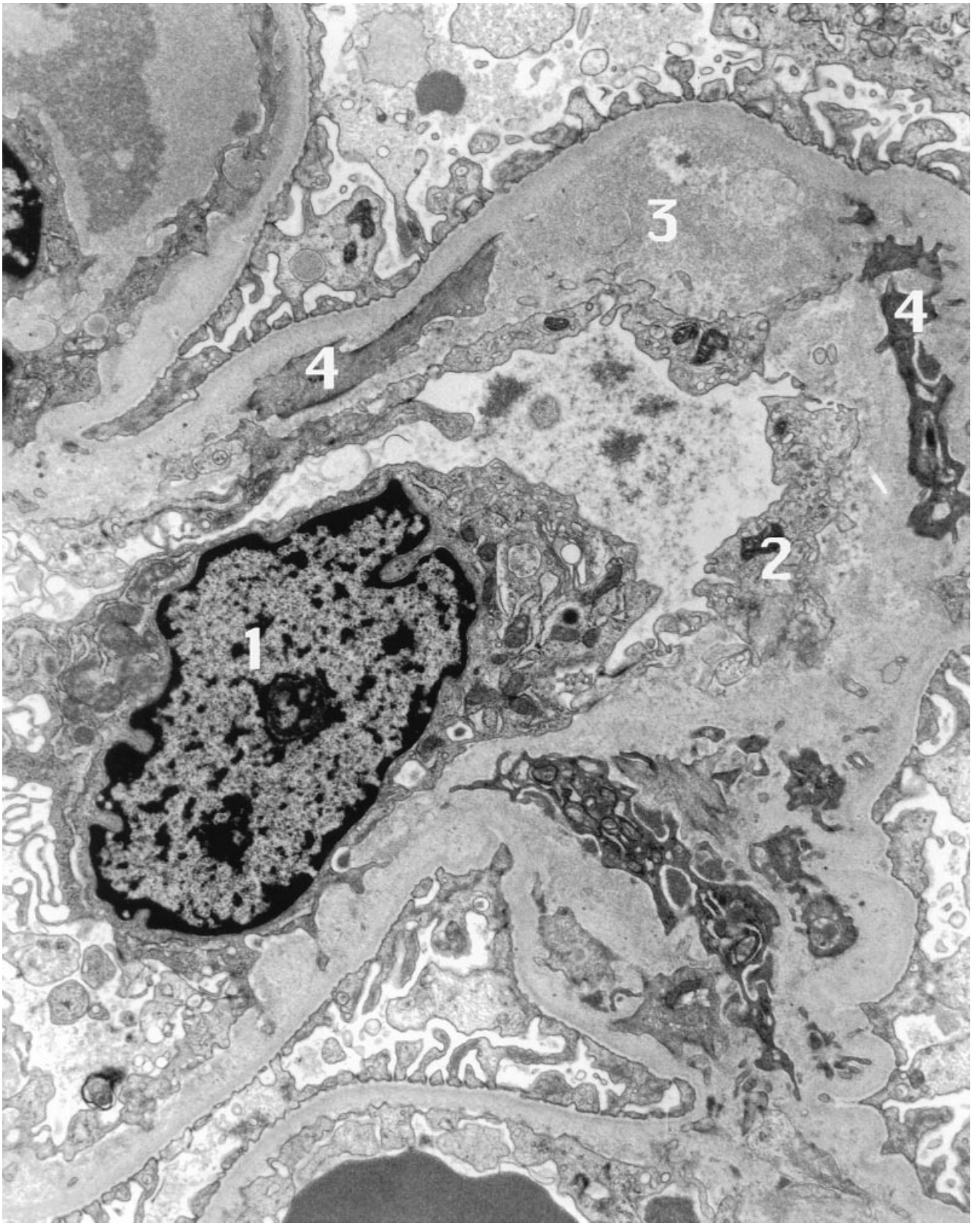

Fig. 1. Transmission electron microscopy (×1800) of a representative glomerular capillary enumerating pathologic changes associated with pre-eclampsia.

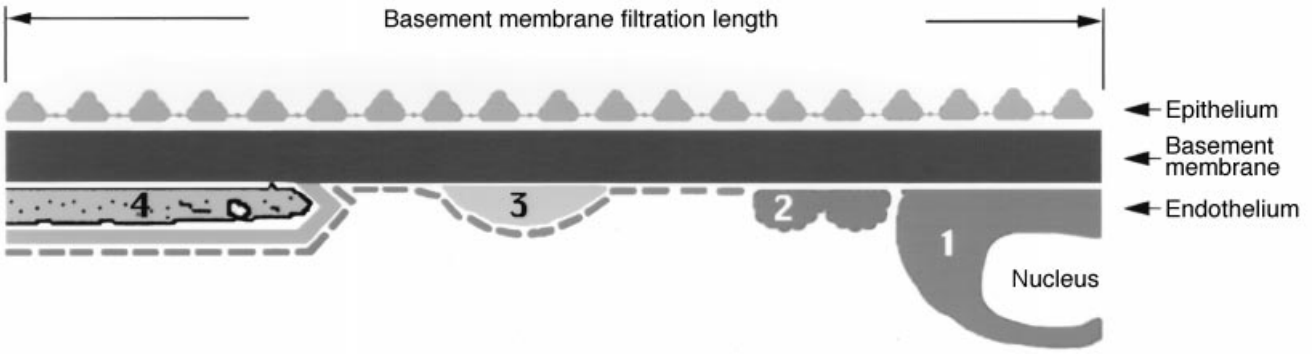

Fig. 2. Schematic depiction of ultrastructural changes in pre-eclampsia. Key: 1, endothelial cell body; 2, swollen, non-fenestrated endothelial cytoplasm; 3, subendothelial fibrinoid deposition; 4, mesangial cell interposition.

Table 3. Morphologic data

	Controls	PET
Glomerular volume (Vg) $\mu m^3 \times 10^6$	3.29 ± 1.19	5.23 ± 2.16[b]
Effective surface density (Sv) $\mu m^2/\mu m^3$	0.100 ± 0.013	0.055 ± 0.017[b]
Filtration slit frequency (FSF) *per mm GBM*	1264 ± 181	1133 ± 163
Thickness GBM (δ_{bm}) *nm*	391 ± 77	403 ± 109
Thickness GC wall (δ_{gcw}) *nm*	391 ± 77	589 ± 136[b]
Fenestral density (n_f) μm^2	49 ± 21	33 ± 15
Fenestral area-to-perimeter (A/P)	0.0096 ± 0.0051	0.0045 ± 0.0011[b]
Fraction GBM occupied by fenestrae (ϵ_f)	0.1370 ± 0.0176	0.046 ± 0.028[b]

For SEM, $N = 7$ gloms in 3 controls and $N = 10$ gloms in 5 PET subjects.
[b] $P < 0.05$ vs. controls

Table 4. Glomerular ultrafiltration capacity

		Pre-eclampsia[a]	
	Controls	Condition A	Condition B
k_{en} *m/s/PA*	1.37×10^{-7}	2.16×10^{-8}	2.16×10^{-8}
k_{bm} *m/s/PA*	4.62×10^{-9}	3.62×10^{-9}	3.08×10^{-9}
k_{ep} *m/s/PA*	6.12×10^{-9}	5.48×10^{-9}	5.48×10^{-9}
Overall k *m/s/PA*	2.58×10^{-9}	1.98×10^{-9}	1.81×10^{-9}
S μm^2	3.28×10^5	2.95×10^5	2.95×10^5
SNK_f *nl/min · mm Hg*	6.78	4.67	4.26

Abbreviations are: k_{en}, k_{bm} and k_{ep}, hydraulic permeabilities of endothelium, basement membrane and epithelium, respectively; overall k is overall hydraulic permeability of the capillary wall; S, effective filtration surface area; SNK_f, single nephron ultrafiltration coefficient.
[a] Condition A assumes that subendothelial fibrinoid is freely permeable to water, whereas condition B assumes that the Darcy permeability of fibrinoid is the same as that of GBM

There was only occasional and patchy broadening of epithelial foot processes in PET, with the result that the filtration slit frequency was not significantly reduced below control (FSF; Table 3). There was also no significant thickening of the peripheral GBM in PET (δ_{bm}; Table 3). There were, however, extensive dense deposits of fibrinoid material in a subendothelial location (#3, Fig. 2). These resulted in a proportionately greater thickening of the entire filtration pathway (δ_{gcw}) (from fenestral interface to slit diaphragm) in PET versus control, 589 ± 136 versus 391 ± 77 nm, respectively ($P < 0.001$; Table 3). Ten glomeruli from five subjects with PET were captured *en face* on their endothelial aspect in scanning electron photomicrographs. Similar photographs of seven glomeruli from the last three kidney donors in this series provided control values (Fig. 3). Judged by a number density of 33 ± 15 versus 49 ± 21 per μm^2, fenestral density was lower in PET than controls (Table 3). A smaller area-to-perimeter ratio attested to a reduction in endothelial fenestral size in PET versus control (Table 3). Together, reduced fenestral density and size in PET resulted in a smaller fraction of GBM occupied by fenestrae (ϵ_f) than in controls. This phenomenon is clearly visible by inspection of the digitized tracings that are taken from a control (left) and a representative subject with PET (right, Fig. 3). Whereas ϵ_f closely approximated 0.16 in all control glomeruli, it was uniformly reduced in glomeruli from the subjects with PET, averaging only 0.046, and varying between 0.014 and 0.087 (Table 3; $P < 0.001$).

Computed filtration capacity

The single nephron ultrafiltration coefficient (SNK_f) and its determinants are summarized in Table 4. SNK_f has been calculated from the mean group, rather than individual values of its structural determinants. This is because only subsets of each group had fenestral density and dimensions assessed by scanning EM (*vide supra*). As shown, endothelial permeability (k_{en}) was substantially reduced and epithelial permeability (k_{ep}) slightly lower in PET than in controls. Basement membrane permeability in PET was depressed below control by 22 or 33%, depending on whether fibrinoid is freely permeable to water (condition A) or has a K_D similar to glomerular basement membrane (Condition B; Table 4). From equation (5), we calculate that overall k in PET was reduced below control not less than 23% (Condition A) or more likely by 30% (Condition B), which is respectively 1.81 versus 2.5×10^{-1} m/s/PA (Table 4). In Condition B, approximately 50% of the reduction was attributable to the fenestral changes, 30% to

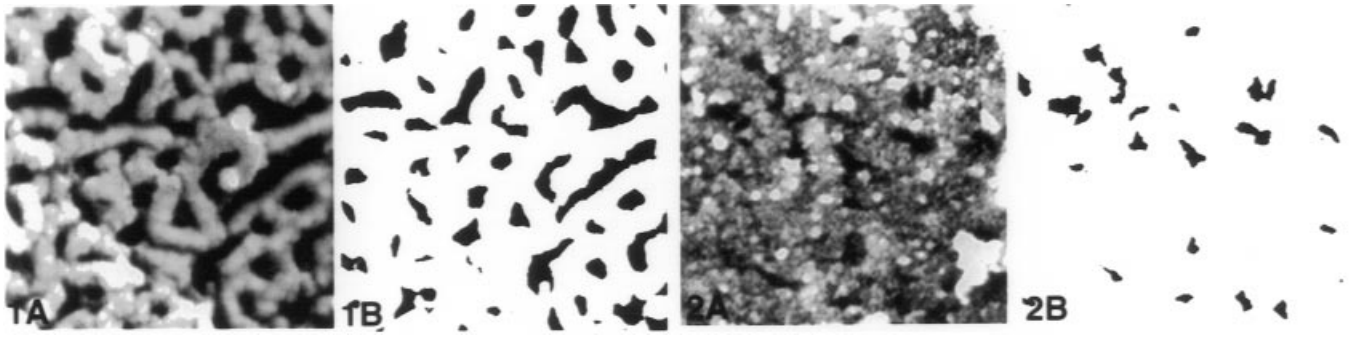

Fig. 3. Scanning electron microscopy and digitized tracings of fenestrae in control (*1A and 1B*) and subjects with pre-eclampsia (*2A and 2B*).

the thickening of the GBM and glomerular capillary wall, and 20% to the reduction in filtration slit frequency. In contrast, effective filtration surface area (S) was only slightly reduced versus controls in PET (Table 4). This reflects the fact that in PET, there were offsetting effects on this quantity of reduced surface density and enhanced glomerular volume (Table 3). From the product of S and k we compute that SNK_f in controls averaged 6.78 nl/(min · mm Hg). The corresponding value in PET was substantially lower at 4.26 to 4.67 nl/(min · mm Hg). Provided that condition B applies, we note that the reduction in estimated SNK_f in PET is by 37% (Table 4), a change that is remarkably similar to the corresponding reduction of 39% in observed GFR in this disorder (Table 2).

DISCUSSION

Not one of the 13 consecutive patients suffering from PET in the present study manifested azotemia. This is not surprising considering that their GFR of 91 ± 25 was only slightly lower than the non-gravid value for healthy women, which in our laboratory is 106 ± 15 ml/min/1.73 m^2. When pregnancy-related hyperfiltration is taken into account, however, it becomes evident that the GFR in our subjects with PET was reduced fully 40% below the appropriate control level (Table 2). Our morphometric analysis of glomeruli suggests that an important, and perhaps predominant reason for the hypofiltration in PET is impaired hydraulic permeability of glomerular capillary walls, owing mainly to reductions in fenestral density and size, and to the accumulation beneath the endothelial monolayer of fibrinoid deposits.

Although the histopathological alterations of glomeruli in PET have been recognized for more than half a century [1], recent investigators of this disorder have largely ignored the possibility that glomerular capillary wall dysfunction could be responsible for its manifestations. Based largely on *in vitro* study of the fetoplacental circulation, authors of current reviews have implied that the glomerular injury of PET is hemodynamic in nature. An increase in renovascular resistance owing to an imbalance favoring vasoconstrictor over vasodilator influences has been held responsible [1–3, 5]. A recent body of evidence has pointed to a central pathogenetic role for diminished activity of the L-arginine-nitric oxide pathway [2, 5, 33, 34]. Indeed, chronic administration of a nitric oxide synthase inhibitor during the third trimester of pregnancy has gained currency as an experimental model of PET in the rat. It results in functional changes that resemble PET, including hypertension, proteinuria, depression of renal plasma flow and GFR, retardation of fetal growth and increased fetal mortality [33, 35, 36]. Whether or not these functional abnormalities are accompanied by typical abnormalities of glomerular morphology, however, has not been reported to date.

In keeping with enhanced vasoconstrictor or diminished vasodilator influences, renovascular resistance was numerically higher in our PET than in our control group, albeit not significantly so (120 ± 46 vs. 92 ± 18 mm Hg · min · $liter^{-1}$, respectively). This trend did not result in a lower glomerular perfusion rate (RPF; Table 2), but could have depressed GFR by lowering glomerular perfusion pressure, and hence the glomerular transcapillary hydraulic pressure difference (ΔP). It seems doubtful that ΔP depression could have made a major contribution to the observed hypofiltration in PET, however. One reason for doubt is that mean arterial pressure in PET exceeded the control value by 23 mm Hg (Table 1). Given the insignificant trend to higher renovascular resistance in PET than controls, it is difficult to envisage a selective increase in preglomerular segmental resistance of sufficient magnitude to prevent some fraction of the excess in arterial pressure from being transmitted into glomerular capillaries. These findings suggest that efforts to directly alter renal plasma flow, such as by infusion of fluids or plasma expanders or by use of vasodilators, may not be beneficial in this disease process.

By making the conservative assumption that ΔP in PET is the same as in controls, and assuming further that the value for ΔP in each group approximates 40 mm Hg [22, 25], we have used the measured values for GFR, renal plasma flow, and π_A to compute group values for two-kidney K_f from the ultrafiltration model of Deen et al [32]. The two-kidney K_f so calculated averaged only 4.8 ± 2.0 in PET versus 8.6 ±

2.8 ml/(min · mm Hg) in controls, respectively ($P < 0.001$). The 44% depression of the hypothetical two-kidney K_f in PET, as calculated from physiological determinations, is reassuringly similar to the corresponding 37% depression of single nephron K_f in PET, as calculated by a morphometric approach (Table 4). The accord between the two independent approaches for estimating K_f suggests to us that K_f depression is indeed the predominant cause of hypofiltration in PET, and that it is unnecessary to invoke a substantial role for simultaneous depression of ΔP in this disorder.

We wish to point out that the morphometric approach used to calculate single nephron K_f in the present study has limitations. For example, we are forced to assume glomerular shrinkage factors owing to immersion fixation and paraffin embedding, so as to calculate glomerular volume. To the extent that shrinkage may vary according to the experimental conditions, the precision with which we have calculated glomerular volume, and hence S, is likely to be limited. Similarly, our computation of k depends on several assumptions that are difficult to validate. Examples include our assumption that the dimensions of apertures in the slit diaphragm and the Darcy permeability of the GBM are the same as in the rat. Even more problematic is that ~30% of glomerular capillary wall thickness in PET is comprised of subendothelial fibrinoid material, for which no *in vitro* estimate of the Darcy permeability is available. In an earlier analysis of k in normal individuals and nephrotic subjects with membranous or minimal change nephropathy, we have shown that extrapolation of the above-mentioned rat values to the hydrodynamic model is unlikely to introduce major errors [19]. The sensitivity analysis used in the present study also suggests that variations in the Darcy permeability of the "non-GBM" fibrinoid fraction of the glomerular capillary wall are unlikely to introduce major errors in the computation of k. We submit, therefore, that whereas the actual values that we have computed for single nephron K_f are likely to be of limited precision, the relative differences in computed K_f values between the PET and control groups of the present study are likely to be real.

A novel, but not surprising result of our analysis is that it points to impairment of k as an important, and perhaps predominant K_f-lowering phenomenon in this common form of glomerular endothelial injury. Studies in the healthy rat indicate that the GBM and the epithelial filtration slit diaphragms each account for approximately 50% of resistance to water flow across the normal glomerular capillary wall [25]. Because of its large and numerous fenestrae the endothelial monolayer accounts for only 1 to 2% of transmural resistance [25]. A reduction in filtration slit frequency, owing to broadening and effacement of foot processes, is the major cause of impaired k in glomerular injuries that are accompanied by nephrotic range proteinuria [19]. Filtration slit frequency was essentially normal in the present study, however. Instead, the density and size of endothelial fenestrae was sufficiently reduced to permit the endothelial layer to account for ~9% of resistance to water flow. Even more important in curtailing water flow is the fact that access to the basement membrane was limited by the fenestral changes, such that the fraction of GBM occupied by fenestrae was reduced below normal by 72%. As a result, basement membrane resistance ($1/k_{bm}$, equation 5) was increased along with endothelial resistance. The presence in the subendothelial space of fibrinoid deposits, along with modest thickening of the GBM, also served to lengthen the extracellular pathway through which filtrate is formed, and hence to further increase $1/k_{bm}$. Together the aforementioned structural changes in and immediately beneath the endothelial monolayer in PET appear to lower k by ~30%, and to be largely responsible for the diminished K_f.

Whereas a K_f-lowering role for impaired k seems clear cut, it is less obvious whether curtailment of S also serves to lower K_f in PET. On the one hand, we have shown that swollen endothelial cell bodies and interposed mesangial cells impinge on the filtration barrier, thereby lowering filtration surface density (S_v; Figs. 1 and 2). PET is also complicated by a reversible form of focal and segmental hyalinosis and glomerulosclerosis, a phenomenon that can further compromise filtration surface density by obliterating segments of the capillary tuft in affected glomeruli [8, 37, 38]. On the other hand, we have shown that PET is accompanied by glomerular hypertrophy, which serves to offset the reduced filtration surface density, and results in a nearly normal value for actual filtration surface area (Table 4). Worthy of emphasis, however, is that the control values in Tables 3 and 4 are those of non-gravid female kidney donors. Compared to the non-gravid state, pregnancy has been reported to be associated with renal hypertrophy [39]. Should glomeruli share in this process of enlargement, the offsetting effect of the disparity in glomerular volume between PET and our present controls will be smaller or disappear. Under these conditions, actual filtration surface area in PET could be significantly depressed below gravid control values, and contribute substantially to a low K_f in PET. Of interest is the finding of heavy albuminuria despite the absence of measurable deformation of podocytes. Conceivably, impaired charge-selectivity, rather than filtration diaphragm-related impairment of size-selectivity, is responsible for albuminuria in this disorder. This was not assessed in the current study.

We conclude that despite an absence of azotemia, the GFR in PET is substantially depressed. Limitations of available methods for evaluating the determinants of GFR in the human kidney prevent us from determining definitively whether reductions in filtration surface area or filtration pressure contribute to the hypofiltration. However, impairment of hydraulic permeability of glomerular capillary walls, a consequence of changes in and beneath

the endothelial monolayer, is clearly implicated in, and is likely to be the predominant cause of hypofiltration in PET.

ACKNOWLEDGMENTS

The study was supported by grant DK 52876 and DK 20368 from the National Institutes of Health. The performance of differential solute clearances in the General Clinical Research Center at Stanford was supported by NIH grant M01 RR00070.

Reprint requests to Richard A. Lafayette, M.D., Division of Nephrology, 300 Pasteur Drive, Stanford University Medical Center, Stanford, California 94305-5114, USA.

REFERENCES

1. Lyall F, Greer IA: Pre-eclampsia: A multifaceted vascular disorder of pregnancy. *J Hypertens* 12:1339–1345, 1994
2. Roberts JM, Redman CWG: Pre-eclampsia: More than pregnancy-induced hypertension. *Lancet* 341:1447–1451, 1993
3. Seligman SP, Buyon JP, Clancy RM, Young BK, Abramson SB: The role of nitric oxide in the pathogenesis of pre-eclampsia. *Am J Obstet Gynecol* 171:944–948, 1994
4. Brown MA: The physiology of pre-eclampsia. *Clin Exp Pharm Phys* 22:781–791, 1995
5. Noris M, Benigni A, Remuzzi G: The role of vasoactive molecules of endothelial origin in the pathophysiology of normal pregnancy and pregnancy-induced hypertension. *Curr Opin Nephrol Hypertens* 5:347–352, 1996
6. Gaber LW, Spargo BH, Lindheimer MD: Renal pathology in pre-eclampsia. *Bailliere Clin Obst Gynecol* 8:443–468, 1994
7. Sheehan HL: Renal morphology in pre-eclampsia. *Kidney Int* 18:241–452, 1980
8. Kincaid-Smith PS: The renal lesion of pre-eclampsia revisited. *Am J Kidney Dis* 17:144–148, 1991
9. Zuspan FP, Samuels P: Preventing pre-eclampsia. *N Engl J Med* 17:1265–1266, 1993
10. Lindheimer MD, Katz AI: The kidney and hypertension in pregnancy, in *The Kidney*, edited by Brenner BM, Rector FC Jr, Philadelphia, WB Saunders Company, 1991
11. Joint National Committee on Detection, and Treatment of High Blood Pressure: National high blood pressure education program working group report on high blood pressure in pregnancy. *Am J Obstet Gynecol* 163:1689–1712, 1990
12. Sims EAH, Krantz KE: Serial studies of renal function during pregnancy and the puerperium in normal women. *J Clin Invest* 37:1764–1774, 1958
13. Ezimokhai M, Davison JM, Philips PR, Dunlop W: Non-postural serial changes in renal function during the third trimester of normal human pregnancy. *Brit J Obstet Gynecol* 88:465–471, 1981
14. Dunlop W: Serial changes in renal haemodynamics during normal human pregnancy. *Br J Obstet Gynaecol* 88:1–9, 1981
15. de Alvarez RR: Renal glomerulotubular mechanisms during normal pregnancy: I. Glomerular filtration rate, renal plasma flow and creatinine clearance. *Am J Obstet Gynecol* 75:931–944, 1958
16. Shemesh O, Golbetz H, Kriss JP, Myers BD: Limitations of creatinine as a filtration marker in glomerulopathic patients. *Kidney Int* 28:830–383, 1995
17. Battilana C, Zhang H, Olshen R, Wexler L, Myers BD: PAH extraction and the estimation of plasma flow in the diseased human kidney. *Am J Physiol* 30:F726–F733, 1991
18. Canaan-Kühl S, Venkatraman ES, Ernst SIB, Olshen RA, Myers BD: Relationships among protein and albumin concentrations and oncotic pressure in nephrotic plasma. *Am J Physiol* 264:F1052–F1059, 1993
19. Drumond CM, Kristal B, Myers BD, Deen WM: Structural basis for reduced glomerular filtration capacity in nephrotic humans. *J Clin Invest* 94:1187–1195, 1994
20. Shirato I, Tomino Y, Koide H, Sakai T: Fine structure of the glomerular basement membrane of the rat kidney visualized by high-resolution scanning electron microscopy. *Cell Tissue Res* 266:1–10, 1991
21. Weibel ER: *Sterological Methods. Practical Methods of Biological Morphometry*. London, Academic Press, 1979
22. Alejandro V, Scandling JD, Sibley RK, Dafoe D, Alfrey E, Deen W, Myers BD: Mechanisms of filtration failure during post-ischemic injury of the human kidney: A study of the reperfused renal allograft. *J Clin Invest* 95:820–831, 1995
23. Miller PL, Meyer TW: Effects of tissue preparation on glomerular volume and capillary structure in the rat. *Lab Invest* 63:862–866, 1990
24. Jensen EB, Gundersen HJG, Osterby R: Determination of membrane of thickness distribution from orthogonal intercepts. *J Microsc* 115:19–33, 1979
25. Drumond MC, Deen WM: Structural determinants of glomerular capillary hydraulic permeability. *Am J Physiol (Renal Fluid Electrol Physiol)* 35:F1–F12, 1994
26. Roberts M, Lindheimer MD, Davison JM: Alterations in glomerular hemodynamics and barrier function in normal pregnancy: Assessment using neutral dextrans and heteroporous membrane modelling. *Am J Physiol* 270:F338–F343, 1996
27. Nguyen HN, Clark SL, Greenspoon J, Diesfield P, Wu PYK: Peripartum colloid osmotic pressures: Correlation with serum proteins. *J Obstet Gynecol* 68:807–810, 1986
28. Hønger, PE: Intravascular mass of albumin in pre-eclampsia and normal pregnancy. *Scand J Clin Lab Invest* 19:283–287, 1967
29. Hønger PE: Albumin metabolism in normal pregnancy. *Scand J Clin Lab Invest* 21:3–9, 1968
30. Olufemi OS, Whittaker PG, Halliday D, Lind T: Albumin metabolism in fasted subjects during late pregnancy. *Clin Sci* 81:161–168, 1991
31. Whittaker PG, Lind T: The intravascular mass of albumin during human pregnancy: A serial study in normal and diabetic women. *British J Obstet Gynaecol* 100:587–592, 1993
32. Deen WM, Robertson CR, Brenner BM: A model of glomerular ultrafiltration in the rat. *Am J Physiol* 223:1178–1183, 1972
33. Raij L, Baylis C: Glomerular actions of nitric oxide. *Kidney Int* 48:20–32, 1995
34. Morris NH, Eaton BM, Dekker G: Nitric oxide, the endothelium, pregnancy and pre-eclampsia. *Br J Obstet Gynaecol* 103:14–15, 1995, 1996
35. Engels K, Deng A, Samsell L, Hill C, Baylis C: Increased nitric oxide (NO) production in normal pregnancy is resistant to inhibition. (abstract) *J Am Soc Nephrol* 4:548A, 1993
36. Yallampalli C, Garfield R: Inhibition of nitric oxide synthesis in rats during pregnancy produces signs similar to those of pre-eclampsia. *Am J Obstet Gynecol* 169:1316–1320, 1993
37. Nochy D, Heudes D, Glotz R, Lemoine R, Gentric D, Bruneval P, Bariety D: Pre-eclampsia associated focal and segmental glomerulosclerosis and glomerular hypertrophy: A morphometric analysis. *Clin Nephrol* 42:9–17, 1994
38. Nagai Y, Arai H, Wahizawa Y, Ger Y, Tanaka M, Maeda M, Kawamura S: FSGS-like lesions in pre-eclampsia. *Clin Nephrol* 36:134–140, 1991
39. Cietak KA, Newton JR: Serial quantitative maternal nephrosonography in pregnancy. *Brit J Radiol* 58:405–413, 1985